Journal of
Ceramic Science
and Technology

J. Ceram. Sci. Tech., 02 [02] 89-96 (2011)
DOI: 10.4416/JCST2011-00001
available online at: http://www.ceramic-science.com

Properties of 2.5Y-TZP Manufactured from Alumina-Doped Yttria-Coated Pyrogenic Zirconia Nanopowder

F. Kern*

University of Stuttgart, Institute for Manufacturing Technologies of Ceramic Components and Composites, 70569 Stuttgart, Allmandring 7b, Germany

received January 10, 2011; accepted February 25, 2011

Abstract

Y-TZP ceramics are widely used owing to their high strength, toughness and abrasion resistance. In this study, pyrogenic zirconia nanopowders were coated with yttria via the nitrate route and blended with 0.5 vol% alumina. Powders were consolidated by hot pressing at 1200 – 1500 °C. The fine-grain TZP materials produced show high strength of 1 GPa. Despite the high toughness of > 9 MPa·√m and high transformability of > 60 %, the ceramics exhibit aging resistance similar to state-of-the-art co-precipitated 3Y-TZP. The parameters of the Mehl-Avrami-Johnson kinetics indicate that aging of coated 2.5Y-TZP proceeds at similar rate constants but more evenly at lower Avrami exponents, which makes the low-temperature degradation process more controllable and less catastrophic. After stress-induced transformation a new phase was identified in the fracture faces which may be an ordered defect structure formed during fast transformation. The phase was not detected after aging-induced transformation.

Keywords: Zirconia, hot pressing, mechanical properties, microstructure, low-temperature degradation, phase analysis

I. Introduction

Y-TZP has been used for almost three decades for engineering ceramics and biomedical applications owing to its high strength, toughness and abrasion resistance. The excellent mechanical properties at ambient temperature are caused by a stress-induced martensitic transformation from metastable tetragonal to thermodynamically stable monoclinic phase. This transformation is accompanied by volume expansion and shear, which sets the process zone before the crack under compressive stress and retards or prevents further crack growth [1]. Y-TZP is usually produced by co-precipitation from yttria and zirconia salt solutions. Yttria stabilizer levels are set at ~3 mol%. After sintering at ~1400 – 1500 °C, the resulting ceramics contain approximately 20 vol% of cubic together with the desired metastable tetragonal phase [2]. These fine-grain-size 3Y-TZP ceramics can be extremely strong (1000 – 1600 MPa), their toughness is only moderate (4 – 5 MPa·m$^{0.5}$). Improvements in toughness – at the expense of strength and aging resistance – can be obtained by reducing the stabilizer content or sintering to larger grain sizes [3,4]. For biomedical applications these strategies can be fatal, as implants may degrade with time and finally fail, causing severe injuries and re-operating effort [5]. The occurrence of a series of failed implants led to intensified research activities. Today the phenomena taking place during low-temperature degradation (LTD) are basically understood. It is widely accepted that a reduction of grain sizes reduces aging as well as addition of alumina, low stabilizer levels accelerate aging as well as high cubic contents [6,7,8]. New strategies to solve the aging problem in biomedical applications are manifold. Ceria-stabilized zirconia/alumina nanocomposites with attractive strength, high toughness and aging resistance were recently presented and mechanically characterized in detail [9,10]. A large producer of implants completely shifted to a zirconia-toughened alumina material with extremely high strength and aging resistance [11,12]. New Y-TZP materials from yttria-coated zirconia powders with improved toughness were developed and successfully tested [13]. These powders showed good processing characteristics and – even more importantly – very low susceptibility to LTD [14,15]. This development came to a rather abrupt end as soon as coated powders were no longer commercially available. The subject has recently been taken up again, results were, however, somewhat contradictory concerning the toughness values [16,17]. The objective of reducing aging with smaller grain sizes has made the application of ultrafine zirconia powders very interesting as these powders have become affordable nowadays. While first results from small size samples were very promising, difficulties in processing have, however, prevented their use. Samples with low stabilizer contents and small grain sizes showed extreme toughness in indentation tests, this high toughness, however, cannot be reproduced with conservative residual strength methods. Progress in spray granulation and slip casting of nanozirconia which may finally make the manufacturing of larger components possible was recently reported [18,19]. The combination of yttria coating and the use of ultrafine zirconia starting powders have recently been published. 2.5Y-TZP materials show attractive strength and high toughness levels [20]. In this study,

* Corresponding author: frank.kern@ifkb.uni-stuttgart.de

attempts were made to further boost the mechanical properties – of strength and toughness – by means of alumina addition and gain initial results on the aging resistance of the new TZP materials. The raw materials basis and processing conditions were kept constant while the sintering temperature range was extended to obtain a broader overview on the changes in materials characteristics with sintering temperature.

II. Experimental

Pyrogenic zirconia nanopowder (VP-PH, Evonik, Germany) with a crystallite size of 12 nm and a specific surface area of 60 ± 20 m²/g (manufacturer's data) was coated with 2.5 mol% yttria via the nitrate route. The pyrogenic powder is produced by means of flame pyrolysis and thus contains a considerable amount of tetragonal as a result of fast quenching; this tetragonal fraction can be easily removed by annealing [20]. The powder is strongly agglomerated as shown by TEM [21]. 5.25 g yttria (99.9 %, Aldrich, USA) was dissolved in half-concentrated nitric acid to produce an yttrium nitrate solution. 120 g VP-PH were dispersed in 400 ml 2-propanol, the nitrate solution and 500 g 3Y-TZP milling balls measuring 5 mm in diameter were added. The mixture was then transferred into a 1000-ml polyethylene flask and gently milled for 24 h at 5 rpm. After removal of the milling balls, the solvent was evaporated at 140 °C. The solid was then crushed with mortar and pestle and calcined in an alumina crucible at 800 °C in air for 1 h. The resulting powder is strongly agglomerated; it is therefore crushed with mortar and pestle and screened through a 100-µm mesh. To obtain the final feedstock, 0.5 vol% alumina (Sasol APA0.5, d_{50} = 300 nm, S_{BET} = 8 m²/g Ceralox, USA) were added and the blend was attrition-milled in 2-propanol for 2 h with 5-mm-diameter 3Y-TZP balls and again for 3 h with 1-mm-diameter 3Y-TZP balls. Powder conditioning was completed by separation of the milling balls, evaporation at 85 °C overnight and screening through a 100-µm mesh. Two batches of coated powder were required to perform the following experiments. Hot pressing (KCE, Germany) was performed in a boron-nitride-clad graphite die measuring 40 mm in diameter. Two disks were pressed simultaneously.

After evacuation and fast heating with 2 MPa pre-load at 50 K/min to 1050 °C, the samples were pre-densified at this temperature at 30 MPa for 10 min. Then heating to final temperature was completed at 20 K/min. This two-stage process was developed during prior studies to improve the quality of the sintered nanozirconia samples [22].

At final temperature the load was increased to 60 MPa for 1 h dwell. Sintering temperatures were varied from 1200 – 1500 °C in 50 K increments. Cooling was performed in the press by shutting off the heater, filling the furnace chamber with argon and removing the load. Prior to testing, all samples were machined according to a standardized procedure. The samples were first lapped with 15-µm diamond suspension, and then polished with 15, 6 and 1-µm diamond suspension for 30 min each (Struers Rotopol, Germany). Two disks for each parameter set were cut into bars measuring 4 mm in width and ~1.6 mm in thickness. Sides and edges were carefully bevelled and polished with 15-µm diamond suspension. Remaining pieces were kept for hardness testing, XRD and aging experiments. Hardness HV_{10} was measured on five indents with a Vickers indenter (Bareiss, Germany), Microhardness $HV_{0.1}$ and indentation modulus were determined on twelve indents according to the universal hardness method (Fischerscope, Germany). Three-point-bending tests according to DIN EN 6872 on ten specimens were performed with 15 span (Hegewald & Peschke, Germany). Fracture toughness was measured by direct crack measurement of indent sizes and wing crack length on five HV_{10} indents using the calculation models of Niihara (Palmquist crack) and Anstis [23,24]. As indentation methods were recently harshly criticized and to validate the measured data, indentation strength in bending (ISB) tests were performed on five samples using the model of Chantikul [25,26]. For the ISB tests bending bars were indented with a HV_{10} indent. The indent was then turned on the tensile side and the residual strength was determined in the same 3-pt setup.

Microstructures were investigated with SEM (Jeol 5400, Japan) on samples thermally etched at 1200 °C for 10 min in air. Secondary electron images were taken without conducting coating at a low acceleration voltage of 3 kV. Grain sizes were measured on samples of 20000 x magnification on five lines according to the line intercept method [27].

The LTD experiments were conducted with an accelerated aging test at 134 °C in a closed autoclave in water vapour. One hour aging under these conditions corresponds to three to four years *in vivo*. Phase compositions of as-polished and aged samples (1, 3, 10, 30 and 100 h) were determined with XRD (Bruker D8, Germany, CuKα, graphite monochromator) using the calibration curve of Toraya [28]. Peak areas of the monoclinic (-111) and (111) reflexes and the tetragonal (101) reflex were integrated. Parameters of the Mehl-Avrami-Johnson (MAJ) kinetics were calculated by regression analysis. Surface roughness of the aged samples was measured by tactile profilometry of five tracks each in an area of 1.75 × 1.75 mm² of each sample (Mahr, Germany). Roughness was correlated to monoclinic content measured.

III. Results and Discussion

(1) Mechanical characterization

Hardness HV_{10}, microhardness $HV_{0.1}$ and indentation modulus E_{IND} are shown in Fig. 1. HV_{10} varies between 1260 and 1330, the maximum hardness was measured on samples sintered at 1400 °C with falling values at both higher and lower temperatures. Microhardness shows a different trend and does not correlate with macrohardness. The curves have two maxima below and above 1400 °C. It seems that the results of microhardness measurements as well as calculated indentation modulus are strongly influenced by phase transformation during the indentation process. The indentation modulus is systematically too high by approximately 10 % compared with literature data for Young's modulus of Y-TZP, which range between 190 – 230 GPa. One would expect falling microhardness owing to the Hall-Petch correlation with rising sintering temperatures (and thus increasing grain sizes), this, however, is not the case. The initial rise in hardness and stiffness reflects incomplete densification at 1200 °C (98 %

theor. density). Three-point-bending strength is shown in Fig. 2. The strength rises from 1200 – 1300 °C, levels at 1000 MPa and falls back to 820 MPa at 1450 °C. Finally the strength rises to 900 MPa at 1500 °C sintering temperature. The strength is not very spectacular for Y-TZP. What makes the material more attractive is the high toughness coupled with this strength level. Fig. 2 shows the residual strength after a HV_{10} indentation. The nanozirconia material is extremely damage-tolerant compared to a state-of-the-art 3Y-TZP (Tosoh TZ-3Y-E hot pressed at 1450 °C/1 h/60 MPa was tested as a reference, here the bending strength is 1550 MPa but the residual strength is just 240 MPa).

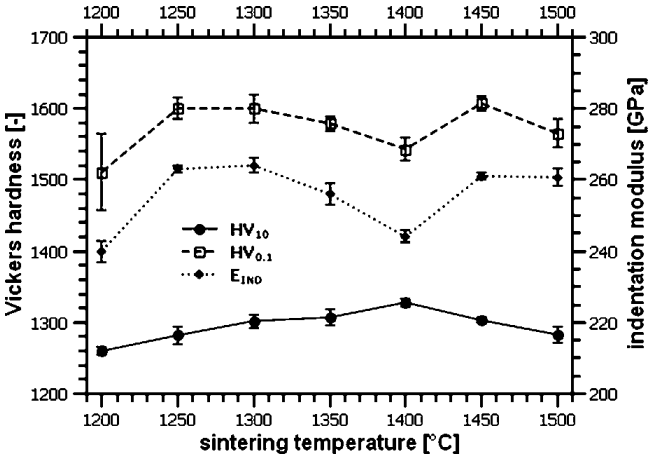

Fig. 1: Hardness HV_{10}, microhardness $HV_{0.1}$ and indentation modulus of 2.5Y-TZP vs. sintering temperature.

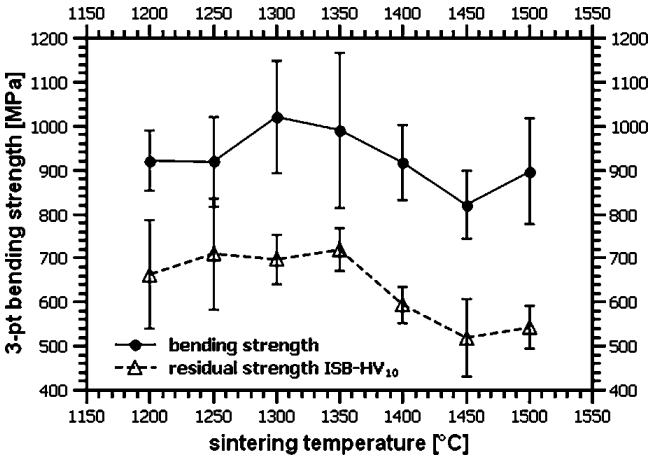

Fig. 2: Three-point-bending strength and residual strength after HV_{10} indentation of 2.5Y-TZP vs. sintering temperature.

Fig. 3 shows the fracture toughness values measured by direct crack measurement and indentation strength in the bending test. Evidently the direct crack measurements interpreted by Niihara's Palmquist crack model are generally too high compared to the ISB tests. The Anstis model leads to more appropriate absolute values. Both indentation models show a sudden breakdown of toughness at 1400 °C. The ISB test, which can be assumed to provide the more realistic toughness values, shows only a decline in toughness. The ISB toughness declines and stays low at higher sintering temperatures while the toughness recovers at higher sintering temperatures in the indentation tests.

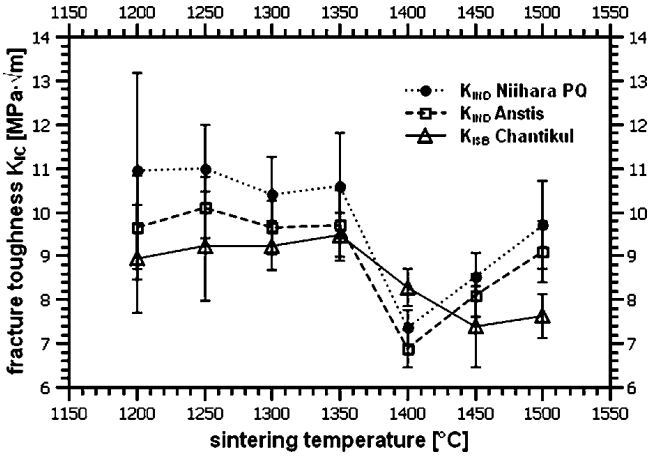

Fig. 3: Fracture toughness of 2.5Y-TZP vs. sintering temperature measured by direct crack measurements and indentation strength in bending.

The combination of very high toughness and high strength shows that the fracture mechanics of the 2.5Y-TZP tested are in the transition range between transformation-dominated and R-curve-dominated behaviour. Swain has shown that extremely high toughness and strength cannot be achieved simultaneously in Y-TZP [29]. In case of ZTA materials it was recently observed that indentation tests provide good results as soon as the toughening mechanism does not change [30]. In the case of this 2.5Y-TZP the shift in reinforcement mechanism could be the elimination of the yttria gradient present at low sintering temperatures < 1350 °C. At higher sintering temperatures the high toughness of coated Y-TZP was attributed to a broadened grain size distribution [17]. High systematic measurement errors were observed in samples sintered at 1200 °C. This can be explained by the fact that low temperatures and thus low thermal activation lead to incomplete and uneven yttria distribution during sintering. This causes non-uniform wing crack lengths of HV_{10} indents in both ISB and direct crack measurements.

(2) Microstructure

Figs. 4a-d show the microstructures of 2.5Y-TZP sintered at 1200, 1300, 1400 and 1500 °C/1 h. Fig. 5 presents the grain sizes measured by the line intercept method. Grain sizes are initially very small, approximately 230 - 250 nm at 1200 – 1250 °C. Then the grains start to grow to reach the limit of biomedical grade TZP (500 nm) at 1400 °C. Finally at 1500 °C, grain sizes of 700 nm are observed. Some residual porosity can be observed in samples sintered at 1200 °C and 1500 °C. The reason for the porosity at low sintering temperature is quite simple, the samples are incompletely densified. There is no obvious reason for the porosity at high temperature; a similar porosity was, however, detected by Singh in previous studies on oversintered 2.5Y-TZP derived from yttria-coated powder. Abnormally large grains as reported by Singh were not detected. A certain broadening of the grain size distribution at temperatures > 1350 °C is obvious. Small grains are completely eliminated at this temperature.

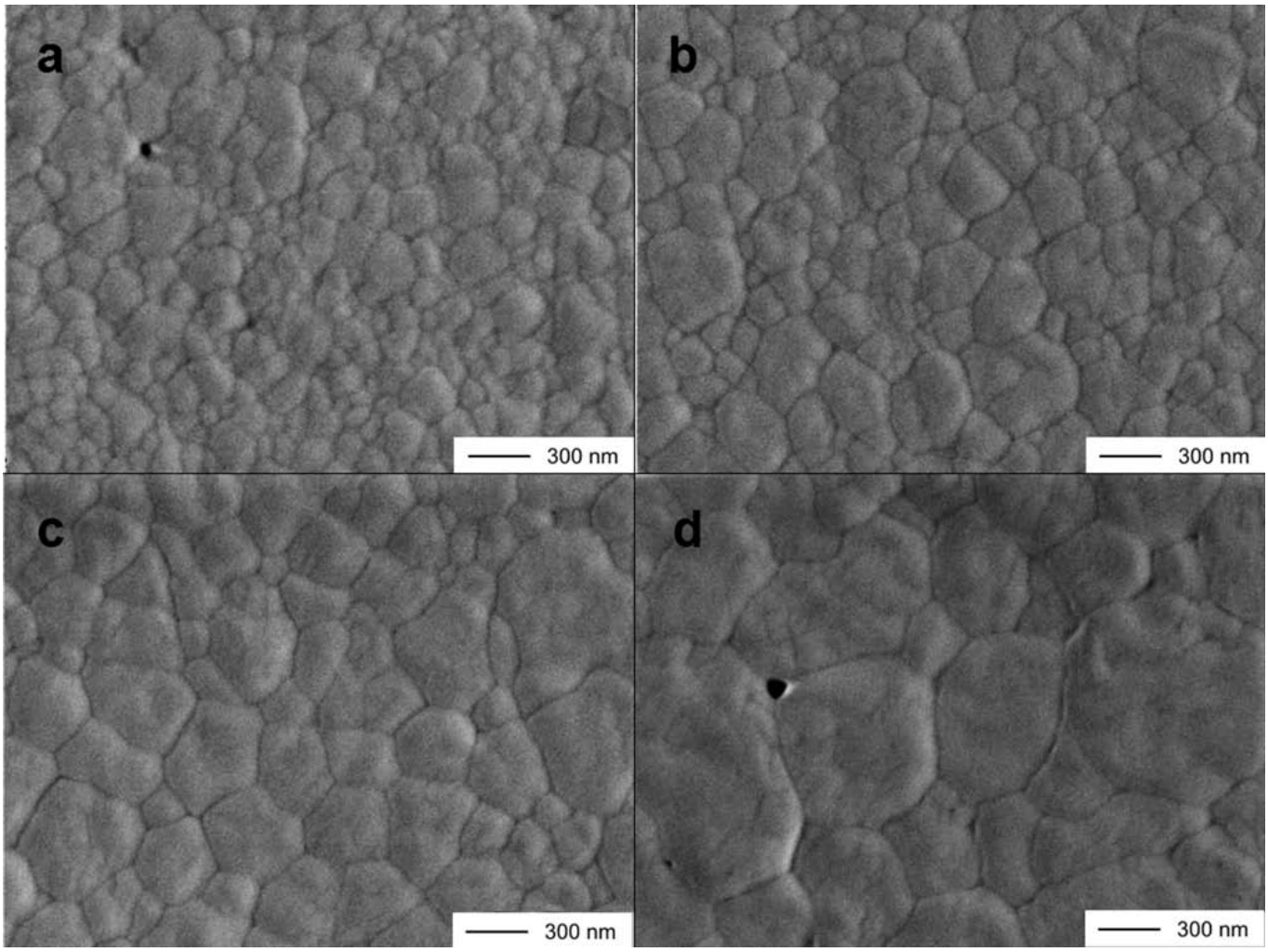

Fig. 4a-d: SEM images of samples sintered at 1200 °C (a), 1300 °C (b), 1400 °C (c), and 1500 °C (d), (thermally etched surfaces 1200 °C/10min/air).

(3) Phase analysis

Phase compositions of polished samples and of fracture phases were determined with XRD. The transformability is defined as the difference of the percentage of monoclinic in fracture surface and polished surface. Fig. 6 shows that the samples are initially almost entirely tetragonal, an exact determination in the < 2 vol% range is almost impossible as the size of the monoclinic reflexes hardly exceeds the noise level. Some transformation may also originate from preparation. Resulting values thus have a very high standard deviation.

Transformability is in the range between 55 and 62 %, an extremely high value for Y-TZP. As transformability is a prerequisite for toughness, it is surprising that the transformability level is similar for all samples despite distinct differences in toughness so that a direct correlation between toughness and transformability cannot be identified.

A closer look at the XRD results of fracture faces revealed another interesting detail. Besides the tetragonal (101) and monoclinic (-111) and (111) peaks, two additional reflexes were detected in the range between 26-33° 2θ, which was scanned for the phase determination. At 28.8 and 29.5° 2θ two very sharp and intensive reflexes were observed. Fig. 7 shows the XRD data of 2.5Y-TZP sintered at 1200 °C. These reflexes were also detected in the XRD patterns of all other fracture faces with the same size ratio but with different intensity. The pattern does not match with known zirconia phases but is very similar to the pattern of $Y_4Zr_3O_{12}$ (δ-phase), however, shifted to lower 2θ values. Thus the material seems to have a rhombohedral symmetry. It is unlikely that the new phase is actually $Y_4Zr_3O_{12}$ as it was not detected in the polished surface and there is neither time nor sufficient thermal activation during transformation to redistribute yttria by diffusion. There is reason to suspect that the new phase is either an intermediate product formed during the martensitic transformation or a by-product of transformation. Results collected by Goff using neutron- and X-ray diffraction can give a hint. The reflexes detected may originate from cation-centred vacancy pairs oriented along a (111) fluorite direction which induce a structural motif: $Zr(1)Zr(2)_6O_{12}V_2$ (1 = central ion, 2 = relaxed nearest neighbours, V = oxygen vacancy), which has the same rhombohedral structure as the δ-phase [31]. These structural motifs are usually short-range defect structures with a diameter of up to 150 nm. Goff's results were confirmed by Elshof based on measurement

of differential capacity [32]. The reason for the pile-up of these defect structures in the vicinity of the growing crack is yet unclear and not the subject of this study. The ordered defect structure in the fracture faces may be stabilized by high local compressive stresses, which prevents its complete transformation to the thermodynamically stable monoclinic phase. The phase was not observed in aged surfaces of the same degree of transformation and seems to be only formed by stress-induced transformation. Further detailed research on this phenomenon is required to validate these *a priori* statements.

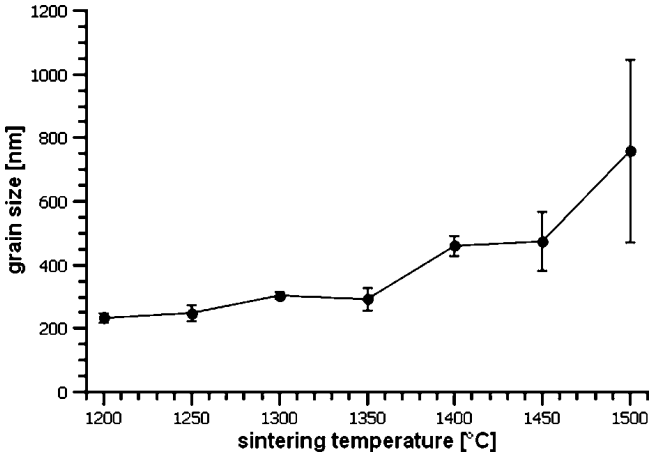

Fig. 5: Grain sizes determined by line intercept method vs. sintering temperature

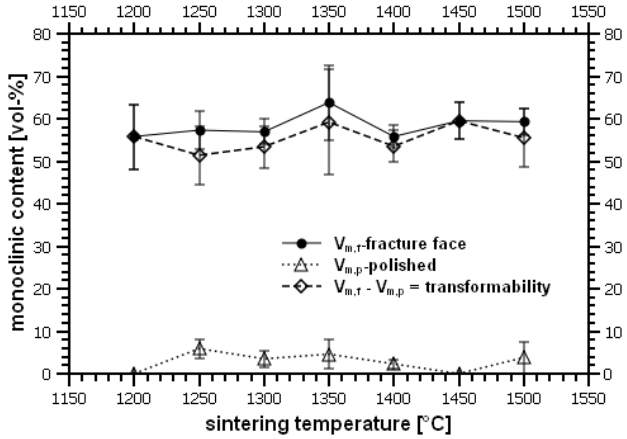

Fig. 6: Monoclinic content in polished surfaces and fracture surfaces and resulting transformability for 2.5Y-TZP vs. sintering temperature.

(4) Low-temperature degradation

The evolution of monoclinic phase formation with aging time at 134 °C is shown in Fig. 8. A continuous rise in monoclinic content can be observed. While the degradation is relatively moderate up to 10 h, it becomes more severe at longer aging times. At 100 h the transformation is almost complete and approaches the maximum of 88 vol% identified by Chevalier [5]. No macroscopic failure except for a freckled surface is observed. The aging characteristics show that the material is not invulnerable to aging as the coated 2.8 Y-TZP investigated by Picconi [15]. It is also not prone to rapid degradation as may be suspected considering its extreme transformability and high toughness. This 2.5Y-TZP matches the improved aging characteristics of modern alumina-doped 3Y-TZP materials sintered at low temperatures. Chevalier's statement that toughness and susceptibility to aging are strictly coupled – a known fact for co-precipitated powders – does not seem to be so strictly valid for coated Y-TZP [33].

Some correlation between toughness and aging resistance is visible. A correlation between grain size and toughness apparently does not exist. It is interesting to see that the highest aging resistance is observed in the material sintered at 1400 °C, which has the lowest toughness in direct crack measurements. The material sintered at 1200 °C, which has the finest grain size, has the lowest aging resistance. Thus it is not the grain size alone which makes Y-TZP aging-resistant or not, accepted results from co-precipitated zirconia materials may not be easily transferred to materials produced from coated powders. Probably at this low sintering temperature the yttria redistribution is not sufficient and leaves regions of low yttria content and high susceptibility to spontaneous transformation.

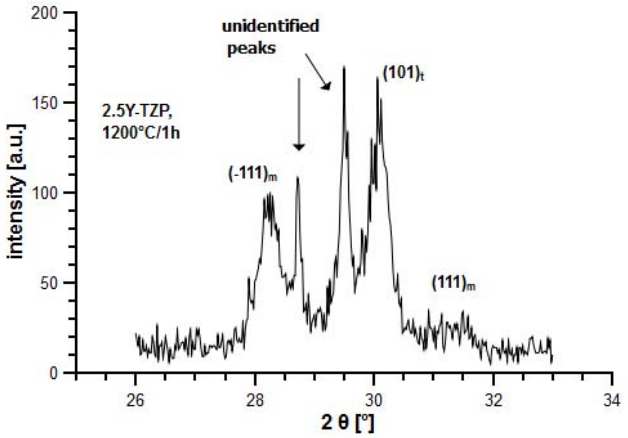

Fig. 7: XRD pattern of the fracture face of 2.5Y-TZP sintered at 1200 °C in the 26-33° 2θ range.

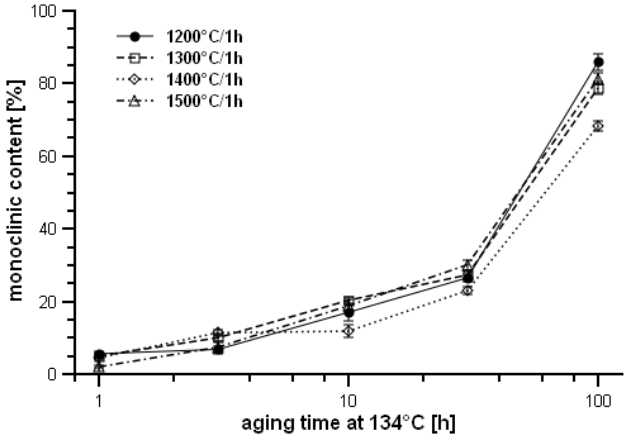

Fig. 8: LTD of 2.5Y-TZP, monoclinic content vs. aging time for TZP sintered at 1200, 1300, 1400 and 1500 °C/1h.

Fig. 9 shows the kinetic constants of the MAJ equation (Eq. 1).

$$f = s \cdot \exp(-k \cdot t)^n \quad (1)$$

f = monoclinic content	[-]
s = maximum transformability (88%)	[-]
k = rate constant	[$^{h-1}$]
t = time	[h]
n = Avrami exponent	[-]

At low turnover the amount of monoclinic formed is mainly dependent on the rate constant, the Avrami exponent n becomes important at higher turnover, thus the sample sintered at 1500 °C with the lowest rate constant ages almost as fast as the samples sintered at 1200 and 1300 °C. Comparing the kinetic parameters to literature data it becomes obvious that the coated 2.5Y-TZP has lower Avrami exponents (0.65-0.9) than 3Y-TZP (~3) but similar exponents as ATZ (1-1.5) [34].

The rate constants are ten times higher than for ATZ but similar to TZP. More experiments will be necessary to measure LTD at different temperatures to determine exact values of activation energies. In this study it was assumed that the activation energy levels reported for co-precipitated TZP are valid also for coated powders.

Fig. 10 shows the roughening of the surface during aging. It is known that phase transformation is accompanied by roughening of the surface as the monoclinic grains occupy more space than the tetragonal grains and stick out of the surface. Monoclinic content and surface roughening can be linearly correlated as shown in Fig. 11. Starting from an initial roughness R_a of 5 nm, which is given by the quality of the preparation, the roughness rises with approximately 0.25 nm/vol% monoclinic. At a roughness R_a of 25 nm full transformation is reached, roughness may then further increase without increasing transformation.

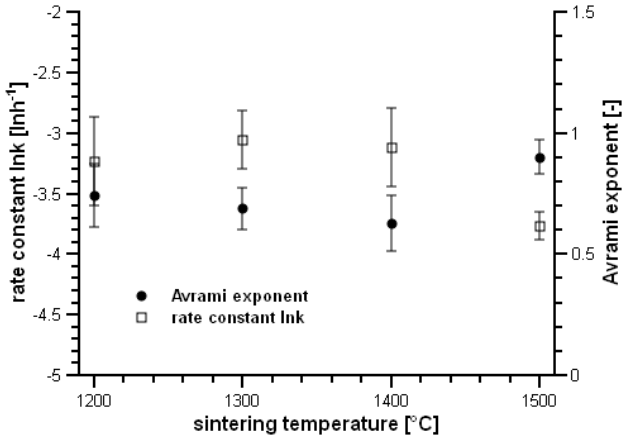

Fig. 9: Kinetic constants of the Mehl Avrami Johnson (MAJ) equation.

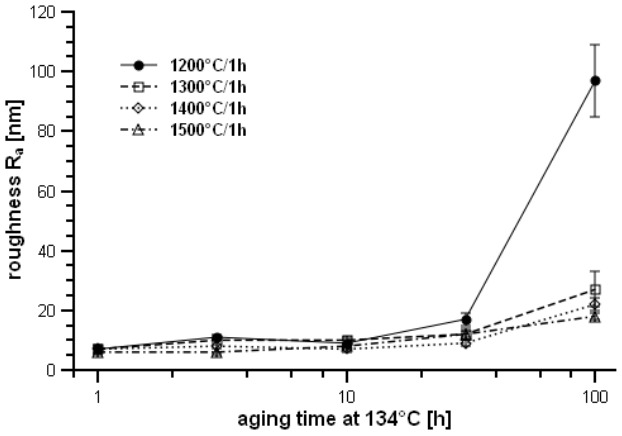

Fig. 10: Surface roughness R_a vs. aging time for 2.5Y-TZP materials sintered at 1200, 1300, 1400 and 1500 °C/1h.

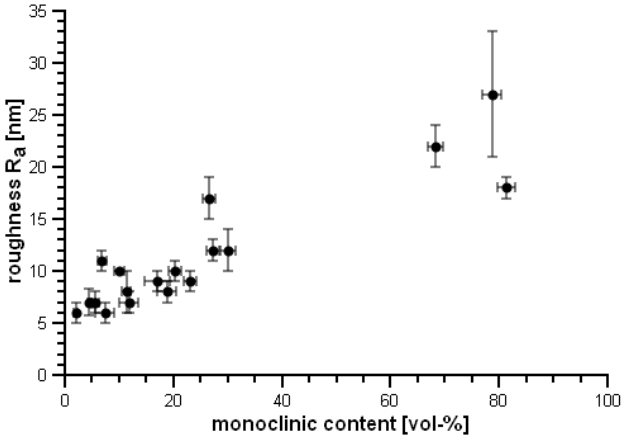

Fig. 11: Surface roughness vs. monoclinic content of 2.5Y-TZP.

IV. Summary and Conclusion

2.5Y-TZP materials doped with 0.5 vol% alumina were manufactured from yttria-coated pyrogenic zirconia nanopowders by hot pressing at sintering temperatures of 1200 – 1500 °C. Resulting materials exhibit extremely high toughness and attractive strength. Full densification is possible at 1250 °C, yielding a material with a fine grain size of 250 nm. In contrast to ultra-tough Y-TZP produced with low stabilizer contents, the indentation toughness values can be reproduced by a residual strength method. The materials are initially completely tetragonal and exhibit extremely high transformability of ~ 60 % which has not yet been reported for Y-TZP of stabilizer levels ≥ 2.5 mol%. LTD is comparable to modern alumina-doped 3Y-TZP which has little transformability and moderate toughness. In some of the fracture faces, evidence for the existence of an ordered defect structure formed during stress-induced martensitic transformation was found. This phenomenon deserves further detailed investigation. For biomedical applications with a tribological load the material produced seems too tough and transformable. Increasing the stabilizer content to 2.6-2.7 mol% yttria may lead to a material with slightly reduced toughness, increased strength and improved aging resistance. Increasing

the alumina content to > 15 vol% to obtain ATZ materials based on the 2.5Y-TZP will also lead to the same results. Together with improved processing methods – hot pressing is just feasible for material characterization – this may lead to interesting materials for biomedical and demanding engineering applications.

References

1 Hannink, R.J., Kelly, P.M., Muddle, B.C.: Transformation toughening in zirconia containing ceramics, *J. Am. Ceram. Soc.,* **83**, [3], 461-87, (2000).

2 Chen, M., Hallstedt, B., Gauckler, L.J.: Thermodynamic modelling of the ZrO_2-$YO_{1.5}$ system, *Solid State Ionics*, **170**, 255-274, (2004).

3 Basu, B., Vleugels, J., Van der Biest, O.: Toughness tailoring in yttria-doped zirconia ceramics, *Mat. Sci. Eng. A*, **380**, 215-221, (2004).

4 Ruiz, L., Readey, M.J: Effect of heat treatment on grain size, phase assemblage, and mechanical properties of 3 mol% Y-TZP, *J.Am.Ceram. Soc.*, **79**, [9], 2331-40, (1996).

5 Chevalier, J., Cales, B., Drouin, J-M.: Low temperature ageing of Y-TZP ceramics, *J. Am. Ceram. Soc.*, **82**, [8], 2150-54, (1999).

6 Ross, I.M., Rainforth, W.M., McComb, D.W., Scott, A.J., Brydson, R.: The role of trace additions of alumina to yttria-tetragonal zirconia polycrystals (Y-TZP), *Scripta Mater.*, **45**, 653-660, (2001).

7 Tsubakino, H., Sonoda, K., Nozato, R.: Martensite transformation behavior during isothermal ageing in partially stabilized zirconia with and without alumina, *J. Mat. Sci. Let.*, **12**, 193-198, (1993).

8 Chevalier, J., Deville, S., Münch, E., Jullian, R., Lair, F.: Critical effect of cubic phase on ageing in 3 mol% yttria-stabilized zirconia ceramics for hip replacement prosthesis, *Biomaterials*, **25**, 5539-5545, (2004).

9 Tanaka, K. et al.: Ce-TZP/Al_2O_3 nanocomposites as a bearing material in total joint replacement, *J. Biomed. Mater. Res.*, **63**, 262-270, (2002).

10 Benzaid, R., Chevalier, J., Saadaoui, M., Fantozzi, G., Nawa, M., Diaz, L.A., Torrecillas, R.: Fracture toughness, strength and slow crack growth in ceria-stabilized zirconia-alumina nanocomposite for medical application, *Biomaterials*, **29**, 3636-3641, (2008)

11 Burger, W., Richter, H.G.: High-strength and toughness alumina matrix composites by transformation toughening and "in situ" platelet reinforcement (ZPTA) – the new generation of bioceramics, *Key Eng. Mat.*, 192-195, 545-548, (2001).

12 Chevalier, J., Grandjean, S., Kuntz, M., Pezzotti G.: On the kinetics and impact of tetragonal to monoclinic transformation in an alumina/zirconia composite for arthoplasty applications, *Biomaterials*, **30**, 5279-5282, (2009).

13 Singh R., Gill, C., Lawson, S., Dransfield, G.P.: Sintering, microstructure and mechanical properties of commercial Y-TZPs, *J. Mat. Sci.*, **31**, 6055- 6062, (1996).

14 Burger, W., Richter, H.G., Piconi, C., Vatteroni, R., Cittadini, A., Boccalari, M.: New Y-TZP powders for medical grade zirconia, *J. Mat. Sci.: Materials in Medicine*, **8**, 113-118, (1997).

15 Picconi, C., Burger, W., Richter, H.G., Cittadini, A., Maccauro, G., Covacci, V., Bruzzese, N., Ricci, G.A., Marmo, E.: Y-TZP ceramics for artificial joint replacements, *Biomaterials*, **19**, 1489-1494, (1998).

16 Yuan, Z.X., Vleugels, J., Van der Biest, O.: Preparation of Y_2O_3-coated ZrO_2 powder by suspension drying, *J. Mat. Sci. Let.*, **19**, 359-361, (2000).

17 Vleugels, J., Yuan, Z.X., Van der Biest, O.: Mechanical properties of Y_2O_3/Al_2O_3-coated Y-TZP ceramics, *J. Eur. Ceram. Soc.*, **22**, 873-881, (2002).

18 Binner, J., Vaidhyanathan, B., Paul, A., Annaporani, K., Raghupathy, B.: Compositional effects in nanostructured yttria-stabilized zirconia, *Int. J. Appl. Ceram. Techn.*, **7**, Suppl s1, E135-E143, (2010).

19 Raghupathy, B.P.C., Binner, J.: Spray Granulation of Nanometric Zirconia Particles, *J. Am. Ceram. Soc.*, no. doi: 10.1111/j.1551-2916.2010.04019.x.

20 Kern, F.: 2.5Y-TZP from Yttria-Coated Pyrogenic Zirconia Nanopowder, *J. Cer. Sci. Tech.*, **1**, [1], 2126, (2010).

21 Nikolay, D., Kollenberg, W., Deller, K., Oswald, M., Tontrup, C.: Manufacturing and properties of ZTA-ceramics with nanoscaled ZrO_2, cfi/Ber. DKG., **83**, [4], E35-E37, (2006).

22 Kern, F., Gadow. R: Proceedings of the 12th European Interregional Conference on Ceramics CIEC 12, University of Mons, Belgium, (2010).

23 Niihara, K.: A fracture mechanics analysis of indentation-induced Palmqvist crack in ceramics, *J. Mat. Sci. Let.*, **2**, 221-223, (1983).

24 Anstis, G.R., Chantikul, P., Lawn, B.R., Marshall, D.B.: A critical evaluation of indentation techniques for measuring fracture toughness: I, Direct crack measurements, *J. Am. Ceram. Soc.*, **64**, [9], 533-538, (1981).

25 Quinn, G.D., Bradt, R.C.: On the indentation fracture toughness test, *J. Am. Ceram. Soc.*, **90**, [3], 673-680, (2007).

26 Chantikul, P., Anstis, G.R., Lawn, B.R., Marshall, D.B.: A critical evaluation of indentation techniques for measuring fracture toughness: II, strength method, *J. Am. Ceram. Soc.*, **64**, [9], 539-543, (1981).

27 Mendelson, M.I.: Average grain size in polycrystalline ceramics, *J. Am. Ceram. Soc.*, **52**, [8], 443-446, (1969).

28 Toraya, H., Yoshimura, M., Somiya, S.: Calibration Curve for Quantitative Analysis of the Monoclinic-Tetragonal ZrO_2 System by X-Ray Diffraction, *J. Am. Ceram. Soc.*, **67**, [6], C119-121, (1984).

29 Swain, M.V., Rose, L.R.F.: Strength limitations in transformation-toughened zirconia alloys, *J. Am. Ceram. Soc.*, **69**, [7], 511-18, (1986).

30 Kern, F.: Microstructure and mechanical properties of hot-pressed alumina – 5 vol% zirconia nanocomposites, *J. Cer. Sci. Tech.*, **2**, [1], 69-74, (2011).

31 Goff, J.P., Hayes, W., Hull, S., Hutchings, M.T., Clausen, K.N.: Defect structure of yttria-stabilized zirconia and its influence on the ionic conductivity at elevated temperatures, *Phys. Rev. B*, **59**, 14202-14219, (1999).

32 Elshof, J.E., Hendriks, M.G.H.M., Bouwmeester, J.M., Verweij, H.: The near surface defect structure of yttria-stabilized zirconia determined by measurement of differential capacity, *J. Mater. Chem.*, **11**, 2564-2571, (2001).

33 Chevalier, J., Gremillard, L., Deville, S.: Low temperature degradation of zirconia and implications to biomedical implants, *Annu. Rev. Mater. Res.*, **37**, 1-32, (2007).

34 Schneider, J., Begand, S., Kriegel, R., Kaps, C., Glien, W., Oberbach, T.: Low-temperature aging behavior of alumina-toughened zirconia, *J. Am. Ceram. Soc.,* **91**, [11], 3613-18, (2008).